

## DESIGN OF VIBRATION-BASED MINIATURE GENERATOR USING PIEZOELECTRIC BENDER

Wei Li<sup>1</sup>, Tzong-Shi Liu<sup>1,\*</sup>, Heng-I Lin<sup>2</sup>, and Yi-Jeng Tsai<sup>3</sup>

<sup>1</sup>Department of Mechanical Engineering

National Chiao Tung University

Hsinchu 30010, Taiwan

<sup>2</sup>Liung Feng Industrial Co., Taipei, Taiwan

<sup>3</sup>Mechanical and Systems Research Laboratories,  
Industrial Technology Research Institute, Hsinchu 31040, Taiwan

E-mail: [tsliu@mail.nctu.edu.tw](mailto:tsliu@mail.nctu.edu.tw)

*Abstract- For the use of green energy and ubiquitous computing, this study investigates miniature electric generators that are constructed with piezoelectric benders. Electric power is generated by vibratory deformation of piezoelectric benders. Three different designs of piezoelectric generators are created and compared in this study by using mechanics analysis. The result shows that the cantilever design yields more power than symmetric and airfoil designs. Experimental results show that generated voltage rises with not only attached point masses, but also the swing frequency of a swing arm, to which the proposed piezoelectric generator is attached. In addition, At 6.5 Hz swing frequency, the maximum power 0.3 $\mu$ W is generated.*

**Index terms:** Miniature Generator, Piezoelectric Bender, Energy Harvesting.

## I. INTRODUCTION

In recent years, several kinds of energy-harvesting designs have been proposed for green energy sources. These designs include acoustic energy collection, electromagnetic and electrostatic power transducers, vibration of piezoelectric materials, etc.

### a. Acoustic energy

Concerning the acoustic energy, or say, sound energy transducers, the electric power is produced by coil vibration in a magnetic field, where the vibration is induced by the variation of the sound pressure. According to Roundy et al. [1], the acoustic energy per unit volume is very small, about  $0.003 \mu\text{W}$  per cubic centimeter at 75 dB and  $0.96 \mu\text{W}$  per cubic centimeter at 100 dB. Therefore, the energy is too small to be utilized for commercial power generation.

### b. Electromagnetic and electrostatic transducers

Williams and Yates [2] pointed out that mechanical energy can be used to generate electric power by a mass-spring-damper system. Mechanical energy due to vibration can be transformed to electric power by any of three kinds of transduction mechanisms including piezoelectric, electromagnetic, and electrostatic devices. And when the mechanical system oscillates at a resonant frequency, there exists the maximum power transformation. Therefore, for performance of the miniature generator, it is important to design a device with resonant frequency coincident with frequencies which human activities result in. For those kinds of miniature electromagnetic or electrostatic generators, the resonant frequency is much higher than that human-being can produce, so we focus on the piezoelectric generator in this paper. A small generator constructed with a high speed permanent magnet generator driven by micro-turbine was used in smart grid energy systems [3]. However, it is not suitable for the environment of vibration.

### c. Vibration of piezoelectric bender

Piezoelectric materials exhibit properties of the electromechanical interaction between the mechanical and electrical states. They can serve as actuators, like [4], due to an inverse piezoelectric effect or as sensors due to a direct piezoelectric effect. The sensors can be made in bulk form depicted in [5] or in the form of thin film to sense cracks [6]. If a lot of electrical charges are generated, electric power may be available. To obtain larger energy density, electric power can be generated by the strain change of a piezoelectric bender. The strain

change is caused by deformation of the piezoelectric bender. Some kinematic conditions, such as vibration or deformation, will change the strain of the piezoelectric bender and hence generate the electric power. As mentioned in [7] and [8], the piezoelectric material can be used in sport shoes. When the compression of the piezoelectric material in the shoes happens, electric power is generated. A wearable embedded system for wirelessly delimiting a hazardous area during emergency was used [9] to alert rescue operators for safety. The power source for this system is an issue. Therefore, Roundy and Wright proposed a power generation method by employing vibration of piezoelectric benders [10].

#### d. Thermoelectric power

Another way to generate power is by the thermoelectric effect. The difference among temperatures makes the thermoelectric device to generate the electric power. It is proposed that power extracted from the human tissue warmth is supplied to a wireless neural recording system implanted in human body [11]. However, it is not suitable for the environment of vibration.

#### e. Amplify, rectify and charge

To use the power generated by the miniature generator, amplify and rectify circuits are needed because the electric current generated is alternating and tiny. Another issue is how to save the electric power, and optimize the efficiency of power transformation from piezoelectric material to an energy storage device, such as rechargeable battery or capacitor. Koutroulis et al. [12] proposed a method for electric energy storage, called step-down converter. Ottman et al. [13, 14] used a full-bridge circuit to rectify the alternating current and store the electric energy. Makihara et al. [15] replaced two diodes in the full-bridge circuit mentioned in [13, 14] by two switches to save the voltage drop by diodes for more energy storage. Sodando et al. [16, 17] used a step-down converter to charge a rechargeable battery and a capacitor directly.

## II. ANALYTICAL MODEL

This paper presents three new designs of the piezoelectric generator. To study the electric power generation, their dynamic models will be analyzed first. Among three designs of the piezoelectric generator, the one that yields the maximum strain will be further investigated in this work. The three designs are depicted in figure 1: (1) cantilever type: a piezoelectric bender is fixed at one end and a point mass  $M$  is attached to the other end. It is a model

similar to [10], but whose rigid body is lumped to a point mass here for comparison purpose. (2) symmetric type: a piezoelectric bender is fixed at two ends while a point mass  $M$  is attached to the middle of the bender. (3) airfoil type: a piezoelectric bender is fixed at its middle and two  $0.5M$  point masses are attached to both ends, respectively, like wings of an airplane.

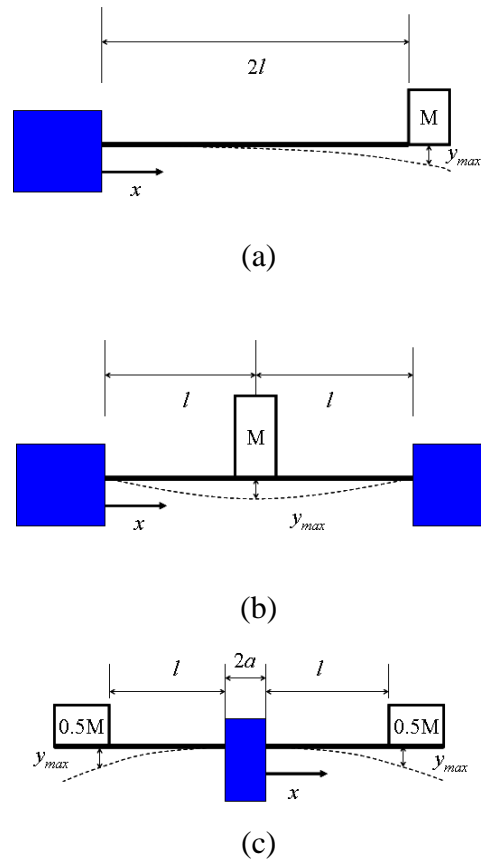


Figure 1. Three designs of miniature piezoelectric generators. (a) Fixed at one end and the point mass attached to the other end (cantilever type). (b) Fixed at two ends and the point mass attached to the middle (symmetric type). (c) Fixed at the middle and two point masses attached to both ends, respectively (airfoil type)

Before studying vibration behavior of these designs, their maximum deflections will be investigated first because the voltage produced by piezoelectric benders is proportional to bending stress. Assume the piezoelectric bender in this study is thin enough to obey the Bernoulli-Euler assumption of the elementary beam theory, the deflection equations can be derived as follows:

a. Deflection of piezoelectric bender

a.i Cantilever type

A cantilever design is shown in figure 1 (a). Assume there is no vibration source acting on the base, by the force and moment equilibrium, the bending moment with respect to  $x$  can be expressed as [18]

$$EI \frac{d^2 y}{dx^2} = -2Mgl + Mgx \quad (1)$$

with boundary conditions

$$\begin{aligned} y(0) &= 0 \\ \left. \frac{dy}{dx} \right|_{x=0} &= 0 \\ EI \left. \frac{d^3 y}{dx^3} \right|_{x=2l} &= Mg \end{aligned} \quad (2)$$

where  $E$  is the elastic modulus of the piezoelectric bender,  $I$  is the moment of inertia of the bender,  $M$  is the mass of the point mass, and  $2l$  is the bender length. Substituting Equation (1) into Equation (2) yields deflection in terms of position  $x$ :

$$y(x) = \frac{Mg}{6EI} (x^3 - 6lx^2) \text{ for } 0 \leq x \leq 2l \quad (3)$$

As a consequence, the maximum deflection occurs at the end attached with a point mass and is written as

$$y_{\max} = \frac{8Mgl^3}{3EI} \quad (4)$$

#### a.ii Symmetric type

A symmetric design with a point mass attached to the middle is shown in figure 1 (b). Assume there is no vibration source acting on the base, the bending moment with respect to  $x$  can be expressed as

$$EI \frac{d^2 y}{dx^2} = -\frac{Mgl}{4} + \frac{1}{2}Mgx \quad (5)$$

with boundary conditions concerning deflection  $y$  and slope  $\frac{dy}{dx}$ :

$$\begin{aligned} y(0) &= 0 \\ y(2l) &= 0 \\ \left. \frac{dy}{dx} \right|_{x=0} &= 0 \\ \left. \frac{dy}{dx} \right|_{x=2l} &= 0 \end{aligned} \quad (6)$$

where  $E$  is the elastic modulus of the piezoelectric,  $I$  is the moment or inertia of the piezoelectric,  $M$  is the mass of the point mass,  $g$  is the acceleration of gravity, and  $2l$  is the piezoelectric length. By substituting Equation (5) into Equation (6), the solution can be expressed as

$$y(x) = \frac{Mg}{48EI} (4x^3 - 6lx^2) \text{ for } 0 \leq x \leq l \quad (7)$$

Hence, the maximum deflection occurs at the middle of the bender and is written as

$$y_{\max} = \frac{Mgl^3}{24EI} \quad (8)$$

#### a.iii Airfoil type

Figure 1 (c) depicts a design that consists of two half-length cantilevers in opposite directions and a  $0.5M$  point mass attached to each end. Therefore, the deflection can be expressed as

$$y(x) = \frac{Mg}{12EI} (x^3 - 3lx^2) \text{ for } 0 \leq x \leq l \quad (9)$$

Accordingly, the maximum deflection occurs at ends of two cantilevers and is written as

$$y_{\max} = \frac{Mgl^3}{6EI} \text{ for one side} \quad (10)$$

where  $E$  is the elastic modulus of the piezoelectric,  $I$  is the moment or inertia of the bender,  $M$  is the mass of the point mass, and  $l$  is the length of each cantilever.

Table 1 compares the above three designs, among which the cantilever type generator has the largest deflection  $\frac{8Mgl^3}{3EI}$  and moment  $2Mgl$ . The largest normal stress is along the  $x$  direction.

Table 1: Comparison among three designs of piezoelectric generator

Types	Symmetric	Cantilever	Airfoil (for one side)
$M(x)$	$EI \frac{d^2 y}{dx^2} = -\frac{Mgl}{4} + \frac{1}{2}Mgx$	$EI \frac{d^2 y}{dx^2} = -2Mgl + Mgx$	$EI \frac{d^2 y}{dx^2} = -\frac{Mgl}{2} + \frac{Mgx}{2}$
$M(x)_{\max}$	$M_{\max} = \frac{3}{4}Mgl$	$M_{\max} = 2Mgl$	$M_{\max} = \frac{Mgl}{2}$
$y(x)$	$y(x) = \frac{Mg}{48EI}(4x^3 - 6lx^2)$	$y(x) = \frac{Mg}{6EI}(x^3 - 6lx^2)$	$y(x) = \frac{Mg}{12EI}(x^3 - 3lx^2)$
$y(x)_{\max}$	$y_{\max} = \frac{Mgl^3}{24EI}$	$y_{\max} = \frac{8Mgl^3}{3EI}$	$y_{\max} = \frac{Mgl^3}{6EI}$

In piezoelectric materials, the strain and electric field has the relationship [19]

$$\{\mathbf{S}\} = \{\mathbf{S}_s\} + [\mathbf{d}]^T \{\mathbf{E}\} \quad (11)$$

where  $\{\mathbf{S}\}$  is the strain vector,  $\{\mathbf{S}_s\}$  is the spontaneous strain vector,  $[\mathbf{d}]^T$  is the transpose of the piezoelectric constant matrix and  $\{\mathbf{E}\}$  is the electric field vector. The piezoelectric constant matrix is defined as

$$[\mathbf{d}] = \begin{bmatrix} 0 & 0 & 0 & 0 & d_{15} & 0 \\ 0 & 0 & 0 & d_{24} & 0 & 0 \\ d_{31} & d_{32} & d_{33} & 0 & 0 & 0 \end{bmatrix} \quad (12)$$

where subscript 1 denotes the direction along the long edge of the piezoelectric bender, subscript 2 denotes the direction along the short edge of the bender, and subscript 3 denotes the thickness direction of the bender. In the beam theory [18], the 1 direction represents the x direction while the 3 direction the y direction. Only the strain in the x direction is concerned, whereas strains in the 2 and 3 directions are negligible. If the spontaneous strain is zero, substituting Equation (12) into Equation (11), which reduces to the strain in the x direction and becomes

$$\varepsilon_1 = d_{31} E_3 \quad (13)$$

Since the beam stress is related to the bending moment by [18]

$$\sigma_1(x) = \frac{-M(x)y}{I} \quad (14)$$

where  $\sigma_1$  is the stress in the x direction and  $M$  is the bending moment,  $I$  is the moment or inertia of the bender, and  $y$  is the distance from the neutral plane along the thickness direction of bender. Based on Hooke's law, the stress  $\sigma_1$  and strain  $\varepsilon_1$  are related by

$$\sigma_1 = E \varepsilon_1 \quad (15)$$

where  $E$  is the elastic modulus. Substituting respectively Equations (13) and (14) into Equation (15) leads to

$$\sigma_1 = Ed_{31}E_3 \quad (16)$$

$$\frac{-My}{I} = Ed_{31}E_3 \quad (17)$$

Therefore, the voltage generated from bender structure is proportional to the bending stress and moment. It follows from Table 1 that the cantilever type will yield the largest voltage among the three designs.

Having obtained the deflection response of the three designs, this study further investigates vibration behaviors. Assume the piezoelectric bender in this study is thin enough to obey the Bernoulli-Euler assumption in the beam theory. To compare performances based on the resulting bending moments of three candidate designs, their mechanics models are derived. The magnitude of generated charge depends on bending moment in piezoelectric benders. Therefore, we compare three designs that all possess the point mass, bender length of  $2l$  with the same piezoelectric material.

#### b. Vibration of piezoelectric bender

In energy harvesting, for future portable usage of miniature generators like a wrist watch on walking human arm depicted in figure 2, the piezoelectric generator has to be fixed at two ends A and O in a case as shown in figure 3(b) subject to dynamic excitation such as arm swing.

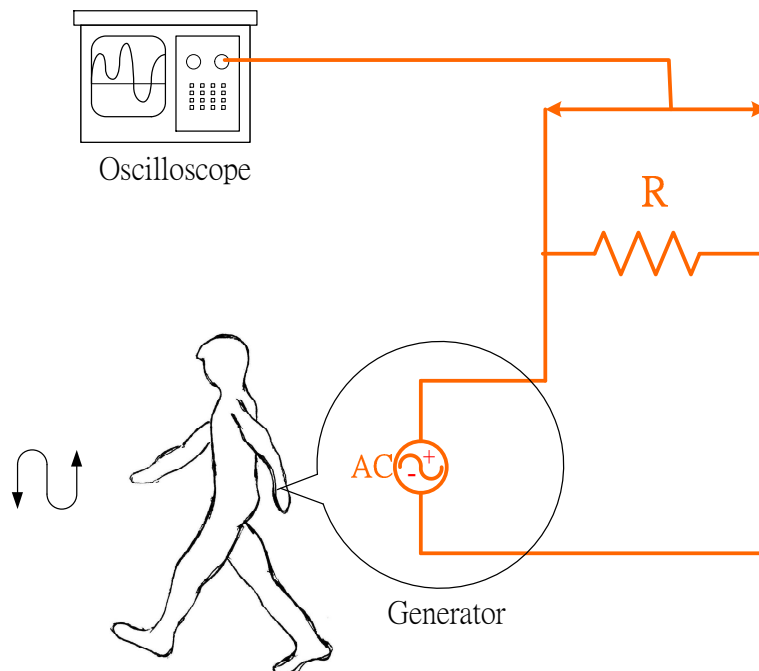
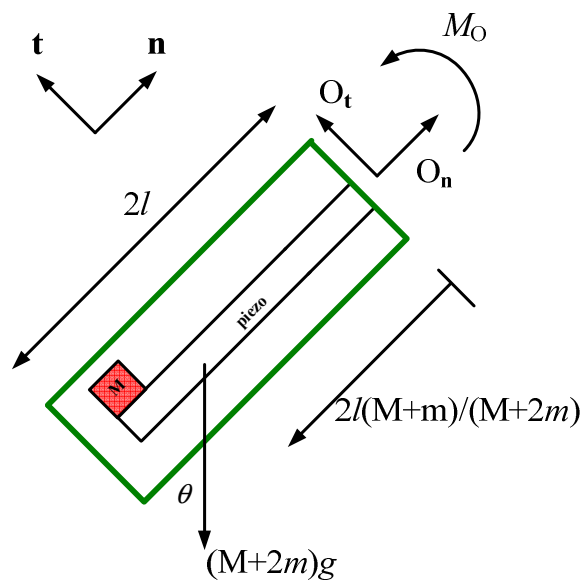
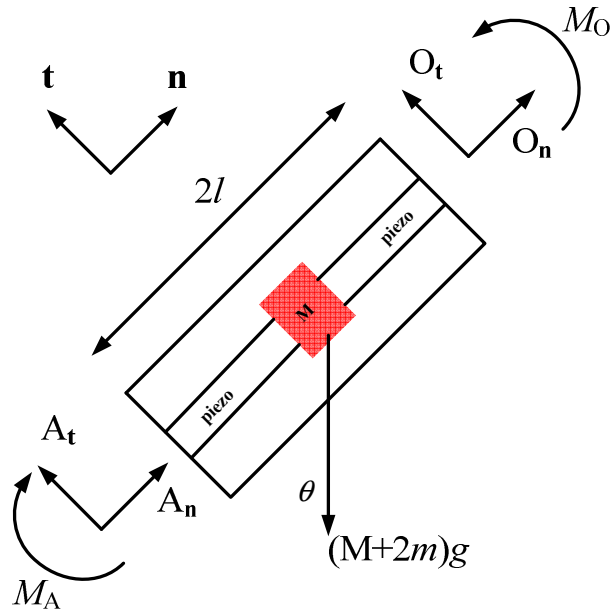


Figure 2. Portable miniature generator subject to environment vibration in a manner similar to wrist watch

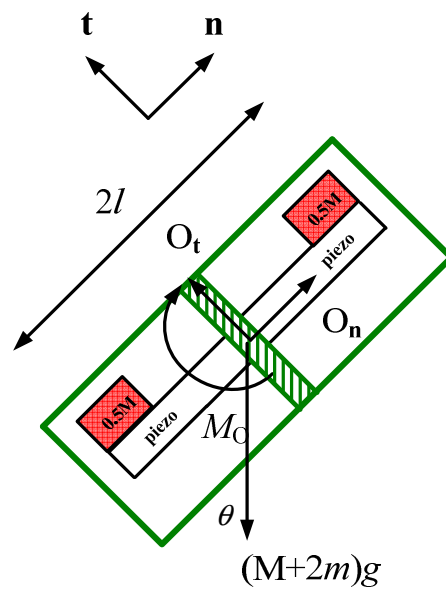
Assume the case as depicted in figures 3 and 4 is endowed with angular acceleration  $\alpha$ , acceleration  $a$ , and oblique angle  $\theta$  with respect to the horizon. Assume that the tangential and normal forces acting on two ends A and O are  $A_t$ ,  $O_t$  and  $A_n$ ,  $O_n$ , respectively. And the moments acting on the two ends are  $M_A$  and  $M_O$ , respectively. Bending moments can be derived from three designs as follows.



(a)

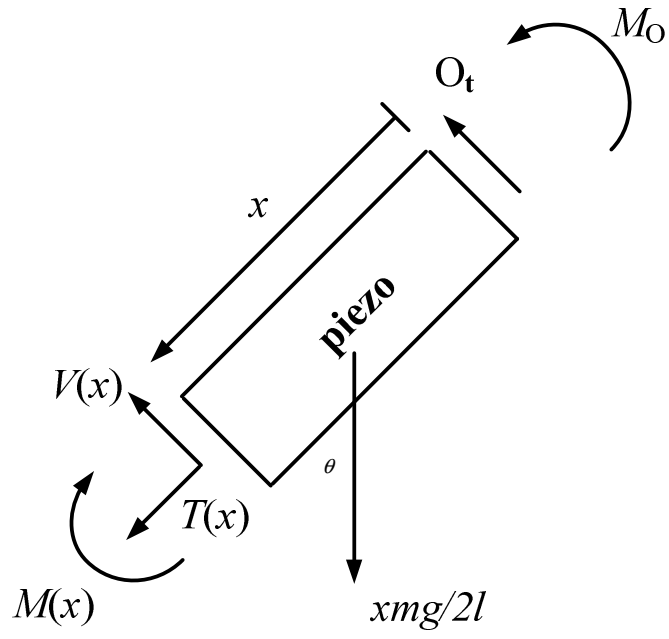


(b)

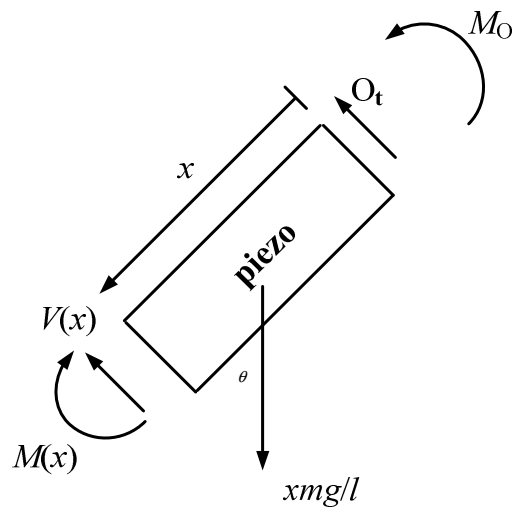


(c)

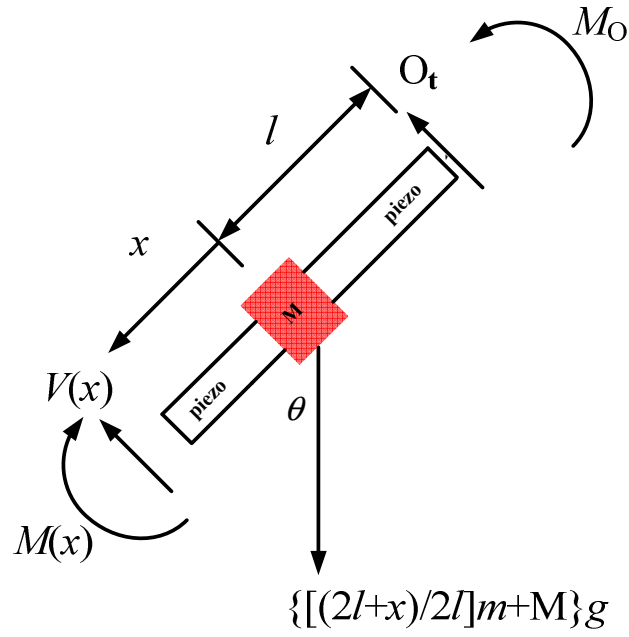
Figure 3. Dynamic models of three designs of miniature piezoelectric generators. (a) Cantilever type, (b) Symmetric type, and (c) Airfoil type



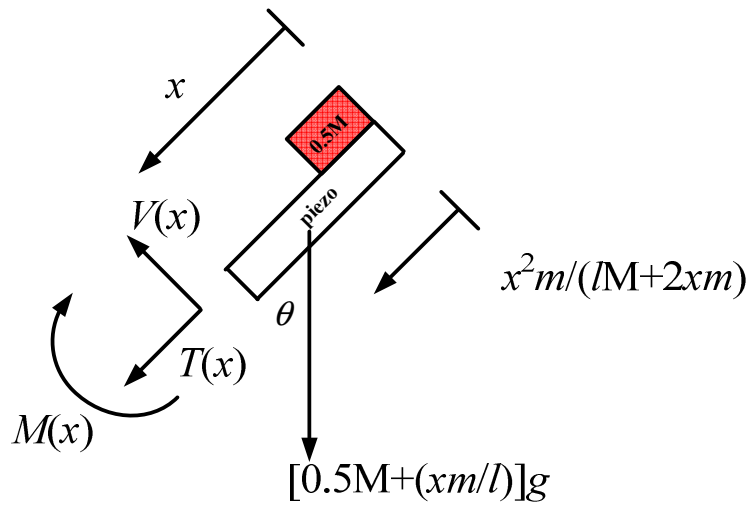
(a)



(b)



(c)



(d)

Figure 4. Free body diagrams of (a) cantilever type, (b) left part of symmetric type without point mass, (c) right part of symmetric type with point mass, and (d) airfoil type

b.i Cantilever type

As shown in figure 3 (a), a cantilever bender is attached to a case. First, the center of mass C is derived as

$$C = \frac{2Ml + 2ml}{M + 2m} = \frac{2l(M + m)}{M + 2m} \quad (18)$$

where  $M$  is the load mass,  $m$  is the bender mass,  $l$  is the length of bender. The moment equation is written as

$$(M + 2m)g \sin \theta \frac{2l(M + m)}{M + 2m} - M_o = \frac{1}{3}(M + 2m)4l^2 \alpha \quad (19)$$

where  $g$  is acceleration of gravity. The force equation in the normal direction is written as

$$O_n - (M + 2m)g \cos \theta = (M + 2m)a_n \quad (20)$$

where  $a_n$  is acceleration in the normal direction and the force equation in the tangential direction is written as

$$(M + 2m)g \sin \theta - O_t = (M + 2m)a_t \quad (21)$$

where  $a_t$  is acceleration in the tangential direction. According to the free body diagram depicted in figure 4 (a), one has

$$(M + 2m)(g \sin \theta - a_t) + V(x) - \frac{x}{l}mg \sin \theta = \frac{x}{l}m \left[ a_t + \left( \frac{2l(M + m)}{M + 2m} - \frac{x}{2} \right) \alpha \right] \quad (22)$$

in the tangential direction and one has

$$(M + 2m)(a_n + g \cos \theta) - \frac{mx}{l}g \cos \theta - T(x) = \frac{mx}{l} \left[ a_n + \left( \frac{2l(M + m)}{M + 2m} - \frac{x}{2} \right) \omega^2 \right] \quad (23)$$

in the normal direction. Similarly, according to the free body diagram depicted in figure 4 (a), the bending moment equation can be expressed as

$$V(x)x + M(x) - \frac{mx}{l}g \sin \theta \frac{x}{2} - M_o = \frac{1}{3} \frac{mx}{l} x^2 \alpha \quad (24)$$

Substituting Equation (19) into the force and moment equations, the bending moment equation can be expressed as

$$M(x) = \frac{1}{3} \frac{2mx}{l} x^2 \alpha - V(x)x + \frac{mx}{l}g \sin \theta \frac{x}{2} + 2l(M + m)g \sin \theta - \frac{4}{3}(M + 2m)l^2 \alpha \quad (25)$$

#### b.ii Symmetric type

As shown in figure 4 (b), in the symmetric design, the bender is attached to a case. In the same manner as the foregoing, the moment equation is derived as

$$O_t l - A_t l + M_o - M_A = \frac{1}{3}(M + 2m)l^2 \alpha \quad (26)$$

and the force equation is written as

$$(M + 2m)g \sin \theta - O_t - A_t = (M + 2m)a_t \quad (27)$$

Assuming  $\delta_o$  and  $\theta_o$  are deflection and deflection angle, respectively at end **O**. There are three effects acting on the end: (1) tangential force  $O_t$ , (2) moment  $M_o$ , and (3) point mass **M** attached to the bender center. Therefore, the deflection and deflection angle at the origin can respectively be written as

$$\delta_o = \frac{8O_t l^3}{3EI} + \frac{2M_o l^2}{EI} - \frac{Mg}{6EI} l^2 (6l - l) = 0 \quad (28)$$

$$\theta_o = \frac{2M_o l}{EI} + \frac{2O_t l^2}{EI} - \frac{Mgl^2}{2EI} = 0 \quad (29)$$

Solving Equations (28) and (29) gives

$$M_o = -\frac{Mgl}{4}, \quad O_t = \frac{Mg}{2}$$

Substituting the above relationships into Equations (26) and (27) leads to

$$A_t = (M + 2m)(g \sin \theta - a_t) - \frac{Mg}{2} \quad (30)$$

$$M_A = \frac{lMg}{4} - l \left[ (M + 2m) \left( g \sin \theta - a_t - \frac{Mg}{2} \right) \right] - \frac{l^2 \alpha}{3} (M + 2m) \quad (31)$$

According to the free body diagram depicted in figure 4 (b), one has

$$M(x) + V(x)x - M_o = \frac{1}{3} \frac{x}{2l} mx^2 \alpha \quad (32)$$

The bending moment equation can be expressed as

$$M(x) = \frac{1}{3} \frac{xm}{2l} x^2 \alpha - \frac{lMg}{4} - V(x)x \quad (33)$$

Similarly, according to the free body diagram depicted in figure 4 (c), one has

$$M(x) + V(x)(l+x) - M_o = \frac{1}{3} \left[ \left( \frac{2l+x}{2l} \right) m + M \right] (l+x)^2 \alpha \quad (34)$$

Thus, the bending moment equation can be expressed as

$$M(x) = \frac{1}{3} \left[ \left( \frac{2l+x}{2l} \right) m + M \right] (l+x)^2 \alpha - V(x)(l+x) - \frac{lMg}{4} \quad (35)$$

### b.iii Airfoil type

In a similar manner, as shown in figures 3 (c) and 4 (d), the bending moment of the airfoil type design can also be derived as

$$M(x) = \left(0.5M + \frac{xm}{l}\right) \left[ g \sin \theta \left( x - \frac{x^2 m}{(lM + 2xm)} \right) + \frac{1}{3} x^2 \alpha \right] \quad (36)$$

Substituting numerical values in Table 2 into Equations (23), (35), and (36) gives Table 3. According to Table 3, the cantilever design will generate the largest dynamic bending moment, hence the largest dynamic deformation. As a consequence, the most electric power will be generated from the cantilever design.

Table 2: Parameters of miniature piezoelectric generator

$m$	0.397g
$m_{\text{point mass}}$	1.057g
$l$	0.042m
$\nu$	0.29
$\rho$	2800Kg/m <sup>3</sup>
$I$	3.78×10 <sup>-14</sup> m <sup>4</sup>
$E$	58GPa

Table 3. Comparison of calculated dynamic bending moments (N-m) among three designs

Symmetric	Cantilever	Airfoil (for one side)
0.0633	0.4203	0.0748

Table 4. Comparison of maximum deflections (m) among three designs

Symmetric	Cantilever	Airfoil (for one side)
0.0017	0.1104	0.0069

### III. NUMERICAL RESULT

For a cantilever beam of the fixed-free end load, the first angular natural frequency is [20]

$$\omega_n = \sqrt{\frac{3EI}{(m_{\text{point mass}} + 0.23 \cdot m)ml^3}} \quad (37)$$

where  $m_{\text{point mass}}$  is the load mass,  $m$  is the bender mass,  $l$  is the length of beam,  $I$  is the area moment of inertia of beam,  $E$  is Young's modulus, and  $\omega_n$  is the angular natural frequency. The above solution can be compared with the cantilever and airfoil types. Moreover, for a fixed-fixed beam of a center load, the first angular natural frequency is [20]

$$\omega_n = 14 \sqrt{\frac{3EI}{(m_{\text{point mass}} + 0.375 \cdot m)l^3}} \quad (38)$$

where  $m_{\text{point mass}}$  is the load mass,  $m$  is the bender mass,  $l$  is the beam length,  $I$  is the area moment of inertia for beam,  $E$  is Young's modulus, and  $\omega_n$  is the angular natural frequency. Using data in Table 2, the natural frequencies are calculated as 44.3, 607.1, and 177.0 Hz for the cantilever type, symmetric type, and airfoil type, respectively. Therefore, the first natural frequency of the cantilever type is closer to the vibration frequency produced by human beings than the other two designs. By using system identification, the actual first natural frequency is 34.7 Hz for the cantilever type, as shown in figure 5. This value is lower than but close to the theoretical value 44.3 Hz, because the theoretical value is derived under the conditions of perfect point mass and homogenous bender. However, the load mass used in system identification is not a rigid body and the bender is indeed a lamination structure. Deflections and natural frequencies of the three designs will be obtained by using MATLAB. To calculate deflections, assume the mass of point mass is 1g. Resultant static deflections of the three designs are shown in Table 4. The ratio of the maximum deflections of the cantilever type to the airfoil type is 16. However, the value of maximum deflection of the airfoil type is for one side only. Hence, the total deflection of the airfoil type should be doubled in view of symmetry. Accordingly, the ratio equals to 8.

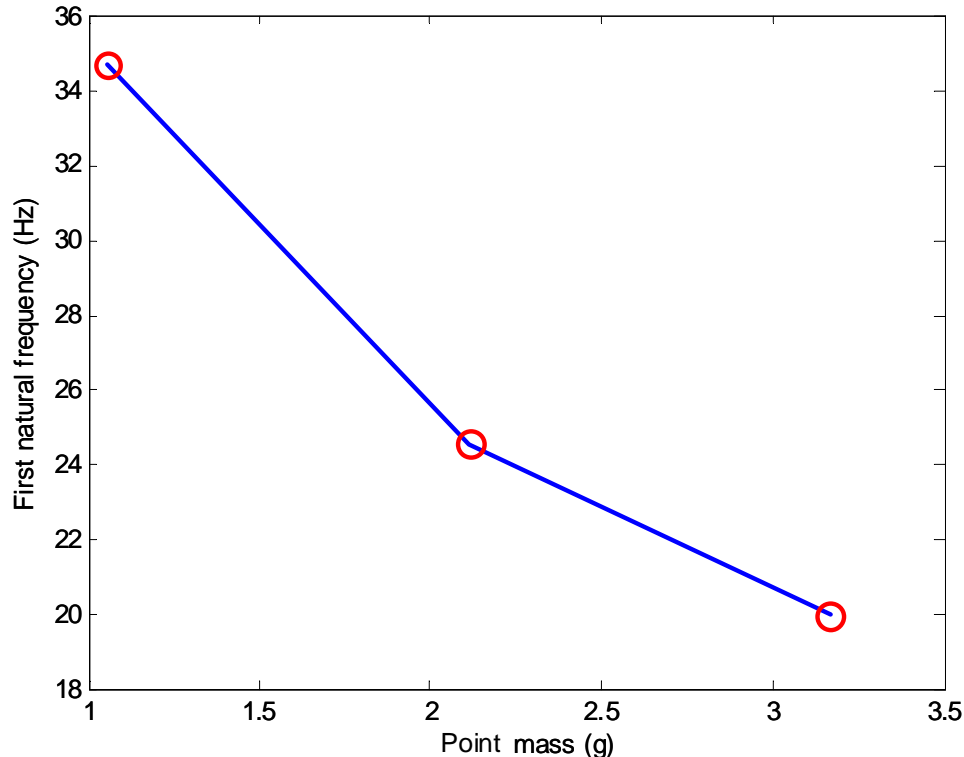


Figure 5. First natural frequency vs. point mass

#### IV. EXPERIMENTAL RESULTS

To verify derivation results summarized in Table 1, an experimental apparatus is set up as shown in figure 6, comparison between cantilever and airfoil types is carried out. A piezoelectric bender is fixed to the end of a swing arm, while the other end of the swing arm is fixed to a motor axis. The piezoelectric bender is fixed to the middle and the end of bender, respectively for cantilever and airfoil types. Using the same condition of motion, root-mean-square voltages measured by an oscilloscope are 0.9494 V and 0.0967 V, respectively for cantilever and airfoil types. And the ratio is about 9.8. In Table 2, the  $y(x)_{\max}$  ratio of the cantilever type to airfoil type is 16; however, the maximum deflection of the airfoil type occurs happens in one side only. Hence, the total deflection of two sides of airfoil type should be doubled, and the  $y(x)_{\max}$  ratio of the cantilever type to airfoil type becomes 8. Therefore, the ratio of maximum voltage and the ratio of maximum deflection are close to each other.

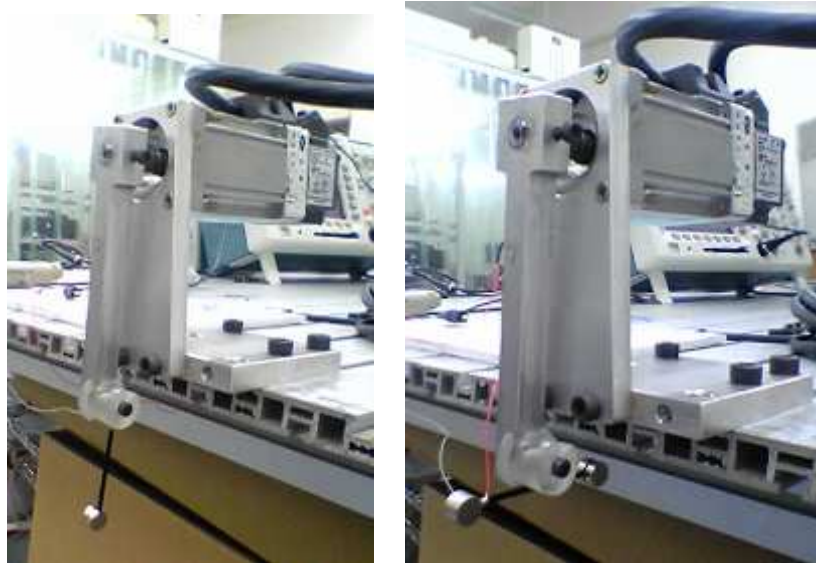


Figure 6. Cantilever type (left) and airfoil type (right) piezoelectric generators attached to swing arm

Vibration of the piezoelectric generator is actuated by a rotational motor, shown in figure 7. The piezoelectric generator is attached to an arm driven by the motor as shown in figure 8. The motor swings back and forth and causes the piezoelectric bender to vibrate. An oscilloscope and a multimeter are utilized to measure voltage and current. The power is obtained from the measured voltage and current. Different point masses, swing frequencies,

and loading resistors are used for the generator. Finally, the electric power generated from the piezoelectric bender is charged to an ultra-capacitor.

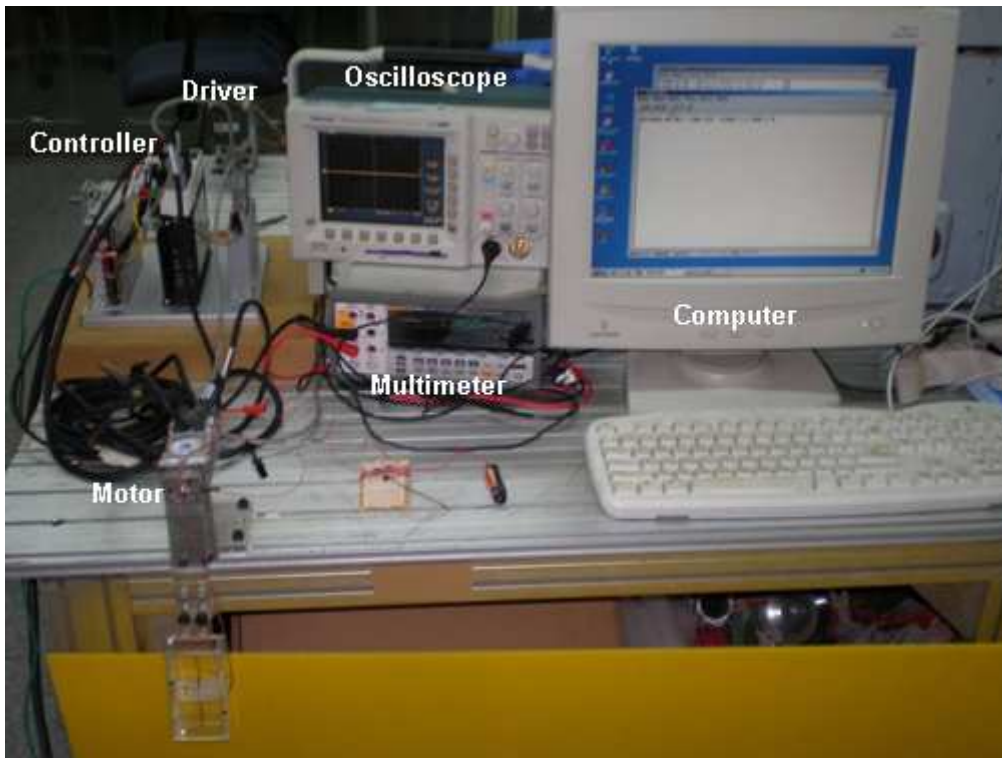


Figure 7. Experimental setup for the piezoelectric generator

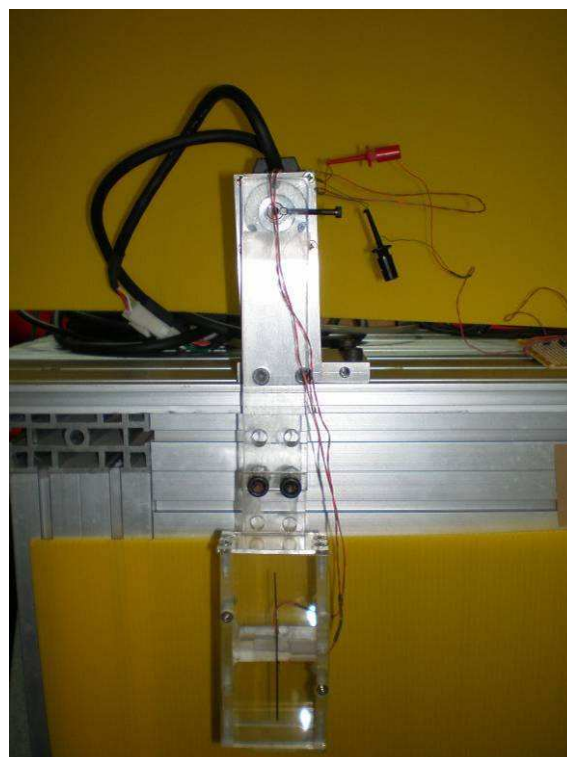


Figure 8. Airfoil type piezoelectric generator attached to swing arm that is driven by motor

Concerning the cantilever type in experiments, the point mass is 0.9g. The swing frequency is about 15Hz without any loading resistor. The voltage generated is about 120mV and the power is about 0.156 $\mu$ W.

In the airfoil type, two different masses are used; namely 2.19g and 3.27g, respectively. Swing frequencies are varied from 1.25Hz to 7.5Hz to simulate the arm swing of the human being. Loading resistances from 2K $\Omega$  to 100K $\Omega$  are used. The voltage generated with different masses and swing frequencies are shown in figure 9. The maximum root-mean-square voltage 2.89V appears with the larger mass 3.27g at 7.5Hz swing frequency. The power generated with different loading resistances and swing frequencies are shown in figure 10. The maximum power 0.3 $\mu$ W appears with 50K $\Omega$  resistance at 6.5Hz.

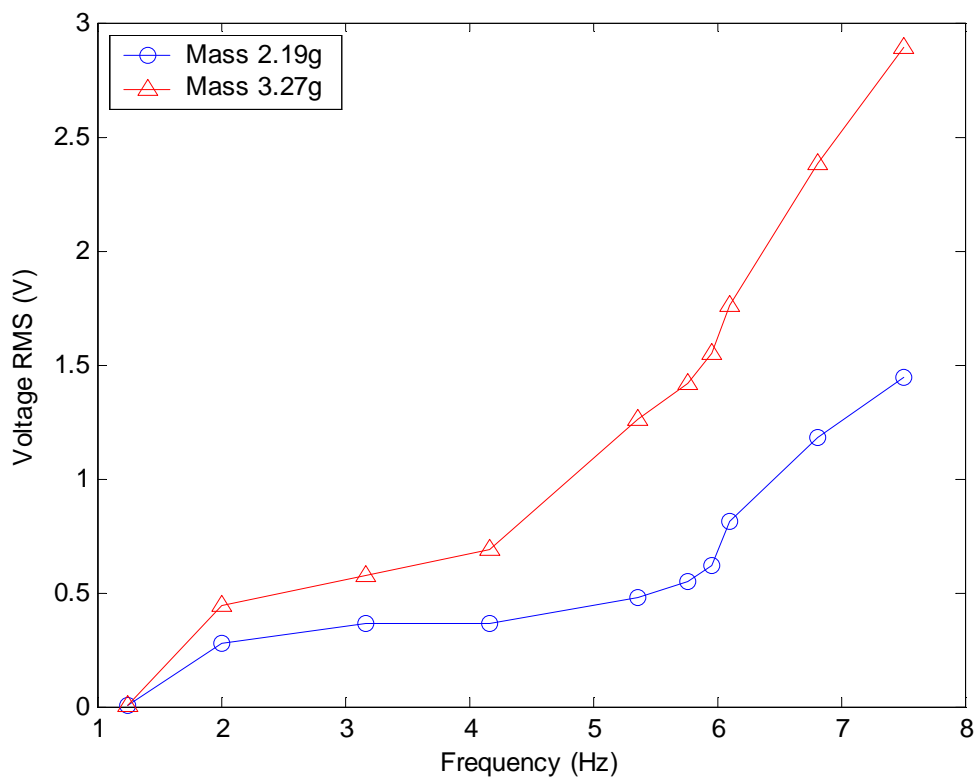


Figure 9. Comparison of voltages with different swing frequencies and point masses

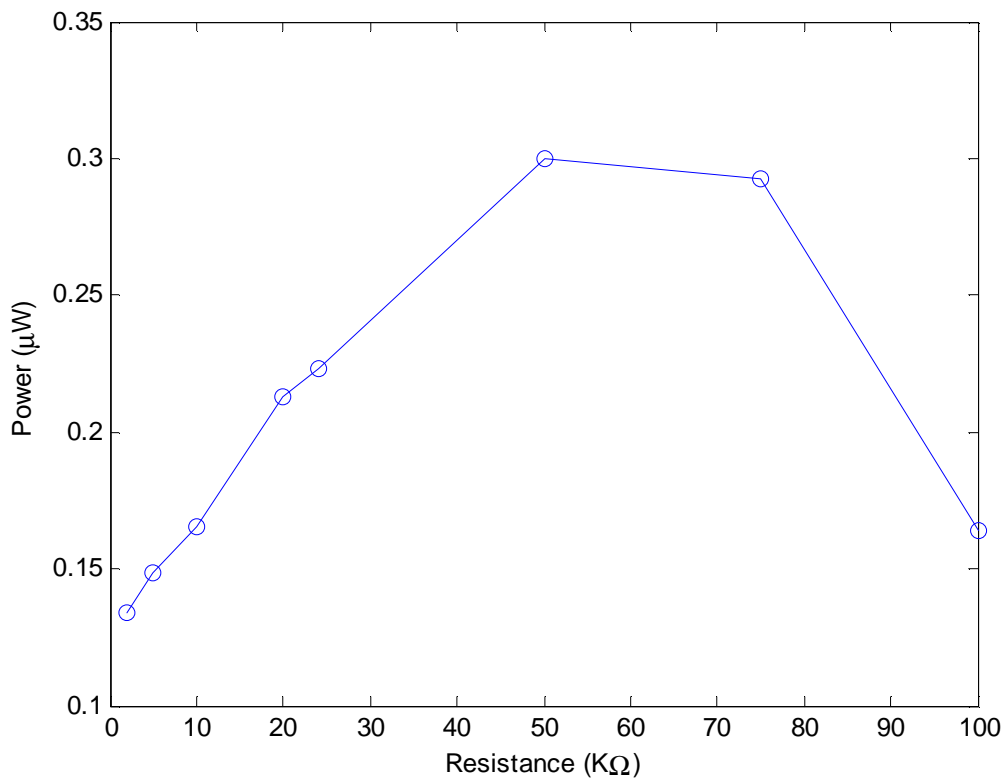


Figure 10. Generated power with different loading resistors

## V. CONCLUSION

The cantilever type is the best design among three piezoelectric generators. However, the natural frequency of the piezoelectric bender is about 110Hz, and it can be reduced to about 20Hz when a 3.17g point mass is attached to the end of piezoelectric bender. Therefore, the resonance of the piezoelectric bender will be easier to occur in the ambient vibration source of human being. Experimental results show that generated voltage rises with not only attached point masses, but also the swing frequency of a swing arm, to which the proposed piezoelectric generator is attached. In addition, at 6.5Hz with 50KΩ loading resistor, the maximum power 0.3μW is generated.

## VI. ACKNOWLEDGEMENTS

This work was supported by National Science Council in Taiwan, R.O.C. under Grant No. NSC96-2221-E009-146.

## REFERENCES

- [1] S. Roundy, P. K. Wright and K. S. J. Pister, Micro-Electrostatic “Vibration-to-Electricity Converters”, ASME International Mechanical Engineering Congress & Exposition, vol. 18, pp.1823-1830. 2002.
- [2] C. B. Williams and R. B. Yates, “Analysis of a Micro-Electric Generator for Microsystems”, Sensors and Actuators, vol. 52, pp. 8-11, 1996.
- [3] A. E. Shahat, A. Keyhani and H. E. Shewy, “Micro-generator Design for Smart Grid System”, International Journal on Smart Sensing and Intelligent Systems, vol. 3, no. 2, pp. 176-216, June 2010.
- [4] S. Neduncheliyan, M. Umapathy and D. Ezhilarasi, “Simultaneous Periodic Output Feedback Control for Piezoelectric Actuated Structures Using Interval Methods”, International Journal on Smart Sensing and Intelligent Systems, vol. 2, no. 3, pp. 417-431, September 2009.
- [5] V. T. Rathod and D. R. Mahapatra, “Lamb Wave Based Monitoring of Plate-Stiffener Debonding Using a Circular Array of Piezoelectric Sensors”, International Journal on Smart Sensing and Intelligent Systems, vol. 3, no. 1, pp. 27-44, March 2010.
- [6] E. Matsumoto and Y. Komagome, “Intelligent Structural Elements Covered by Piezoelectric High-Polymer Film”, International Journal on Smart Sensing and Intelligent Systems, vol. 1, no. 2, pp. 420-429, June 2008.
- [7] T. Starner, “Human-powered Wearable Computing”, IBM Systems Journal, vol. 35, pp. 1898-1902, 1996.
- [8] N. S. Shenck and J. A. Paradiso, “Energy Scavenging with Shoe-Mounted Piezoelectrics”, IEEE Micro, vol. 21, pp. 30-42, 2001.
- [9] C. Alippi and C. Galperti, “An Embedded Wireless System for Estimating the Exposition Risk in First Emergency Management”, International Journal on Smart Sensing and Intelligent Systems, vol. 1, no. 3, pp. 592-612, September 2008.
- [10] S. Roundy and P. K. Wright, “A Piezoelectric Vibration Based Generator for Wireless Electronics”, Smart Materials and Structures, vol. 13, pp 1131-1142, 2004.
- [11] G. B. Hmida, A. L. Ekuakille, A. Kachouri, H. Ghariani, and A. Trotta, “Extracting Electric Power from Human Body for Supplying Neural Recording System”, International Journal on Smart Sensing and Intelligent Systems, vol. 2, no. 2, pp. 229-245, June 2009.

- [12] E. Koutroulis, K. Kalaitzakis and N. C. Voulgaris, “Development of a Microcontroller-Based Photovoltaic Maximum Power Point Tracking Control System”, *IEEE Transactions on Power Electronics*, vol. 16, pp. 46–54, 2001.
- [13] G. K. Ottman, H. F. Hofmann, A. C. Bhatt and G. A. Lesieutre, “Adaptive Piezoelectric Energy Harvesting Circuit for Wireless Remote Power Supply”, *IEEE Transactions on Power Electronics*, vol. 17, pp. 669–676, 2002.
- [14] G. K. Ottman, H. F. Hofmann and G. A. Lesieutre, “Optimized Piezoelectric Energy Harvesting Circuit Using Step-Down Converter in Discontinuous Conduction Mode”, *IEEE Transactions on Power Electronics*, vol. 18, pp. 696–703, 2003.
- [15] K. Makihara, J. Onoda and T. Miyakawa, “Low Energy Dissipation Electric Circuit for Energy Harvesting”, *Smart Materials and Structures*, vol. 15, pp. 1493–1498, 2006.
- [16] H. A. Sodando, D. J. Inman and G. Park, “Comparison of Piezoelectric Energy Harvesting Devices for Recharging Batteries”, *Journal of Intelligent Material Systems and Structures*, vol. 16, pp. 799–807, 2005.
- [17] H. A. Sodando, D. J. Inman and G. Park, “Generation and Storage of Electricity form Power Harvesting Device”, *Journal of Intelligent Material Systems and Structures*, vol. 16, pp. 67–75, 2005.
- [18] D. R. Cook and C. W. Young, “Advanced Mechanics of Materials”, Macmillan Publishing Company, 1985.
- [19] G. W. Taylor, J. J. Gagnepain, T. R. Meeker, T. Nakamura and L. A. Shuvalov, “Piezoelectricity”, Gordon and Breach, Science Publisher, Inc., 1985.
- [20] C. M. Harris, “Shock and Vibration Handbook”, McGraw Hill 3<sup>rd</sup>, 1987.